ARTICLE

MYC directly transactivates CR2/CD21, the receptor of the Epstein–Barr virus, enhancing the viral infection of Burkitt lymphoma cells

Ester Molina[1,2,7,8], Lucía García-Gutiérrez[1,2,8], Vanessa Junco[1,2], Mercedes Perez-Olivares[3], Virginia G. de Yébenes[4,5], Rosa Blanco[1,2], Laura Quevedo[1,2], Juan C. Acosta[1,2], Ana V. Marín[5], Daniela Ulgiati[6], Ramon Merino[1,2], M. Dolores Delgado[1,2], Ignacio Varela[1,2], José R. Regueiro[5], Ignacio Moreno de Alborán[3], Almudena R. Ramiro[4] and Javier León[1,2]✉

MYC is an oncogenic transcription factor dysregulated in about half of total human tumors. While transcriptomic studies reveal more than 1000 genes regulated by MYC, a much smaller fraction of genes is directly transactivated by MYC. Virtually all Burkitt lymphoma (BL) carry chromosomal translocations involving MYC oncogene. Most endemic BL and a fraction of sporadic BL are associated with Epstein–Barr virus (EBV) infection. The currently accepted mechanism is that EBV is the BL-causing agent inducing MYC translocation. Herein we show that the EBV receptor, *CR2* (also called *CD21*), is a direct MYC target gene. This is based on several pieces of evidence: MYC induces CR2 expression in both proliferating and arrested cells and in the absence of protein synthesis, binds the *CR2* promoter and transactivates *CR2* in an E-box-dependent manner. Moreover, using mice with conditional MYC ablation we show that MYC induces *CR2* in primary B cells. Importantly, modulation of MYC levels directly correlates with EBV's ability of infection in BL cells. Altogether, in contrast to the widely accepted hypothesis for the correlation between EBV and BL, we propose an alternative hypothesis in which MYC dysregulation could be the first event leading to the subsequent EBV infection.

Oncogene (2023) 42:3358–3370; https://doi.org/10.1038/s41388-023-02846-9

INTRODUCTION

MYC is a transcription factor that belongs to the b-HLH-LZ family of proteins and binds DNA as a dimer with MAX. MYC-MAX heterodimers bind to the DNA to consensus sequences called E-boxes (CANNTG motif), present in most MYC target genes [1, 2]. MYC transforms cells modulating functions essential in tumor cell biology as cell cycle progression, energetic metabolism, lipid and nucleotide biosynthesis, protein synthesis, apoptosis and differentiation [1–3]. MYC regulates more than one thousand genes [4–7]. However, the identification of direct MYC target genes is hampered because MYC is a weak transactivator but provokes profound changes in cell physiology. Therefore, many of these genes are regulated not directly by MYC but as a secondary effect of changes induced by MYC. Indeed, only a minority of the genes having MYC bound at the promoter are identified as direct MYC targets (reviewed in [8]).

MYC is dysregulated in about 50% of human malignancies of different types [9, 10] and it is particularly prevalent in lymphoma and leukemia [11, 12]. Burkitt lymphoma (BL) is an aggressive lymphoma originally described in equatorial Africa [13]. It is the most common childhood cancer in areas where malaria is endemic in Africa, Brazil and Papua New Guinea. This BL variant is called endemic BL (eBL) and shows high prevalence in children (5–10 per 10^5 cases/year). Clinically and histologically similar BL occurs in Europe and USA affecting children and adults with much lesser prevalence, a variant called sporadic BL (sBL). A third less common variant is the immunodeficiency-associated BL [14, 15].

BL is believed to originate in the germinal center of lymph nodes, where rapidly dividing B cells undergo somatic hypermutation and class-switch recombination of the immunoglobulin genes. MYC plays a prominent role in germinal center formation [12, 16]. Activation-induced cytidine deaminase (AID) initiates somatic hypermutation and class-switch recombination [17], but it can also induce Ig/MYC translocations [18, 19]. *MYC* is translocated to one of the immunoglobulin *loci* in nearly all BL cases, resulting in aberrant *MYC* expression under the control of the immunoglobulin enhancers. The most frequent translocation occurs into the immunoglobulin heavy chain [t(8;14)(q24;q32)] but it could also be found in the light chain *loci*. Besides *MYC* translocations, 30–50% of BL carry mutations within the MYC gene [15, 20, 21], many of them generating a more stable MYC protein [22].

The Epstein–Barr virus (EBV) is a herpesvirus originally discovered associated with eBL. The global prevalence of EBV in BL patients is around 50% and it is decreasing over the last 20 years.

[1]Instituto de Biomedicina y Biotecnología de Cantabria (IBBTEC), Universidad de Cantabria-CSIC, Santander, Spain. [2]Departamento de Biología Molecular, Universidad de Cantabria, Santander, Spain. [3]Department of Immunology and Oncology, Centro Nacional de Biotecnología (CNB)-CSIC, Madrid, Spain. [4]Centro Nacional de Investigaciones Cardiovasculares-CNIC Carlos III, Madrid, Spain. [5]Department of Immunology, Ophthalmology and ENT, Universidad Complutense, School of Medicine and 12 de Octubre Health Research Institute (imas12), Madrid, Spain. [6]School of Biomedical Sciences, The University of Western Australia, Crawley, WA, Australia. [7]Present address: The Hormel Institute, University of Minnesota, Austin, MN, USA. [8]These authors contributed equally: Ester Molina, Lucía García-Gutiérrez. ✉email: leonj@unican.es

Received: 1 February 2023 Revised: 12 September 2023 Accepted: 18 September 2023
Published online: 29 September 2023

However, while EBV is present in more than 90% of the eBL cases, it is detected in only 1–2% of adults and 30–40% of children with sBL. EBV is also detected in 30–40% of patients with the immunodeficiency-associated BL [14, 23, 24]. EBV establishes a harmless lifelong infection in B cells in over 95% of adults worldwide, and it is associated with infectious mononucleosis [25] and multiple sclerosis [26, 27]. EBV was the first virus described with oncogenic potential due to its association with BL and its ability to transform B cells into immortalized lymphoblastoid cell lines [28]. EBV can display three gene expression programs, called latency programs I, II and III, in which different sets of viral genes are expressed [23, 26, 28]. These genes are involved in processes leading to B cell transformation, such as immortalization [29], resistance to apoptosis [30] and metabolic reprogramming [31].

The most accepted hypothesis to explain the high incidence of EBV in eBL proposes a causative role for EBV. This hypothesis stemmed from the finding of high EBV antibodies titers in sera of African children before the BL diagnosis [32]. This and subsequent reports led to the declaration of EBV as a causative agent of BL by the WHO [33]. EBV, malaria and HIV infection are cofactors that may cooperate with MYC in promoting B cell proliferation in the germinal center by reducing apoptosis or impairing the immune surveillance of the tumor [14, 34, 35]. However, the pathogenic mechanism by which EBV genes promote MYC translocation in BL tumorigenesis is unclear. Furthermore, some data do not fit with the hypothesis of EBV being the cause of BL. EBV infection is absent in the vast majority of the adult sBL cases, while EBV infection is associated with other tumors (e.g., nasopharyngeal carcinoma, gastric cancer, Hodgkin lymphoma, post-transplant lymphoproliferative disease, peripheral T cell lymphoma) where MYC translocation is absent (reviewed in [23, 26, 36]). EBV infects B lymphocytes through a membrane glycoprotein, the complement receptor 2 or CR2 (also termed CD21) [37]. CR2 acts as a co-receptor for B cell receptor (BCR) and is found in a complex with other proteins such as CD19 or CD81 [38].

In this work, we show that MYC directly induces CR2 expression in BL-derived cell lines and primary B cells. Induction of CR2 by MYC overexpression leads to a higher number of EBV-infected cells. Based on this, we propose an alternative mechanism in which the upregulation of MYC due to chromosomal translocation increases the receptor density at the B cell surface, leading to B lymphocytes being more prone to infection by EBV.

RESULTS

MYC downregulation leads to decreased CR2 expression in lymphoma cells

Previous studies on gene expression profiling of K562 leukemia cells revealed *CR2* as one of the genes regulated by MYC (J.C. Acosta, PhD Thesis Dissertation, University of Cantabria, 2005). Given the involvement of MYC in BL, we investigated whether *CR2* could be a novel MYC target gene. Treatment of Raji cells (BL cell line) and Jurkat cells (acute T cell lymphoblastic leukemia cell line) with JQ1, an inhibitor of the bromodomain and extra terminal (BET) family of proteins known to potently inhibit MYC transcription [39], resulted in MYC mRNA downregulation. This was accompanied by a decrease in *CR2* mRNA expression (Fig. 1A). The decrease in MYC and CR2 expression was also detected at the protein level in both cell lines (Fig. 1B). MYC is necessary to maintain cell cycle progression and MYC downregulation is known to arrest proliferation [3]. In agreement, the treatment of Raji and Jurkat cells with increasing concentrations of JQ1 decreased their proliferative capacity in a dose-dependent manner (Supplementary Fig. 1A) and increased the percentage of cells in G_1 phase (Supplementary Fig. 1B). Longer exposure to JQ1 resulted in apoptosis, as shown by annexin V staining (Supplementary Fig. 1C).

To investigate the direct effect of MYC downregulation on *CR2* expression, we asked whether *MYC* silencing led to *CR2* downregulation. We knocked down MYC expression in Raji cells using short-hairpin RNA constructs (shMYC)-containing lentiviral particles (a mixture of two sh constructs targeting human MYC). The results showed that MYC depletion significantly reduced CR2 mRNA and protein levels (Fig. 1C). The rate of cell proliferation was also dramatically reduced upon MYC silencing (Fig. 1D).

It is reported that high MYC levels inhibit the induction of EBV lytic cycle in BL cells [40]. Thus, we asked whether MYC silencing in our Raji cells model can induce EBV lytic cycle. We silenced MYC expression with shMYC lentivirus and determined the expression of viral genes associated with the lytic cycle. The results showed that MYC knockdown resulted in the induction of early-lytic genes as *BZLF1*, *BLLF1* and *BRLF1* (Supplementary Fig. 2). As a positive control, we used 12-O-tetradecanoylphorbol-13-acetate (TPA), reported to induce lytic genes in Raji cells [41].

MYC upregulates *CR2* mRNA expression independently of cell proliferation

The former results can be explained if CR2 expression is linked to the proliferation state of the cell, so it would decrease as a consequence of proliferation arrest in MYC-depleted cells. To address this issue, we used KMycJ cells, a K562-derived cell line with ectopic MYC expression inducible by Zn^{2+} addition [42]. In these cells, JQ1 treatment decreased endogenous *MYC* expression while the addition of Zn^{2+} induced the exogenous MYC (Fig. 2A, C). Total MYC levels did not increase in growing cells treated with Zn^{2+} likely due to a well-known MYC auto-suppression mechanism by which exogenous MYC downregulates endogenous *MYC* levels in most systems, so that total MYC levels do not rise above a certain threshold [43, 44]. The proliferative arrest of KMycJ cells upon JQ1 treatment was not rescued by ectopic MYC expression (Fig. 2B). We found that induction of MYC by Zn^{2+} resulted in the upregulation of *CR2* mRNA levels in JQ1-arrested cells (Fig. 2C). To further confirm that CR2 regulation by MYC is independent of the proliferative state of the cells, we performed a similar experiment but inducing cell cycle arrest with TPA, a drug known to arrest proliferation and dramatically reduce MYC levels in these cells [44]. KMycJ cells were treated with TPA and then the ectopic MYC expression was induced with Zn^{2+}. As shown in Fig. 2D, TPA induced a proliferative arrest that was not rescued by MYC upon Zn^{2+} addition. We found that *CR2* mRNA levels increased upon MYC induction even in TPA-arrested cells (Fig. 2E).

As a parallel approach, we used another K562-derived cell line, Kp27MER, which contains a *CDKN1B* transgene ($p27^{KIP}$) inducible by Zn^{2+} and the chimeric protein MYC-ER which becomes activated by 4-hydroxy-tamoxifen (4HT). $p27^{KIP}$ is a CDK and cell cycle inhibitor and as expected, addition of Zn^{2+} induced p27 expression and inhibited cell proliferation (Fig. 2F). Despite this proliferation arrest, we observed an increase in *CR2* expression after MYC-ER activation (Fig. 2G). As a control, we confirmed the MYC-dependent upregulation of *LDHA*, a bona fide MYC target gene [45]. Taken together, the results suggest that *CR2* induction is an effect of MYC and not a consequence of MYC-mediated proliferation.

MYC directly binds to the *CR2* promoter

Chromatin immunoprecipitation (ChIP)-seq data generated by the ENCODE Consortium (https://genome-euro.ucsc.edu, GRCh37/hg19) predicted two peaks of MYC and MAX occupancy within the proximal region of *CR2* promoter in human B cells (Fig. 3A). There are four canonical E-boxes in the region surrounding the *CR2* transcription start site (TSS), two of which mapped within the promoter near the TSS and the other two within the first intron (Fig. 3B). To confirm MYC binding to *CR2* promoter in BL-derived cells we performed ChIP with an anti-MYC antibody in Raji cells, analyzing different regions of the CR2 promoter and first intron. The results showed enrichment of MYC binding to the proximal region of *CR2* promoter in a region containing two close E-boxes

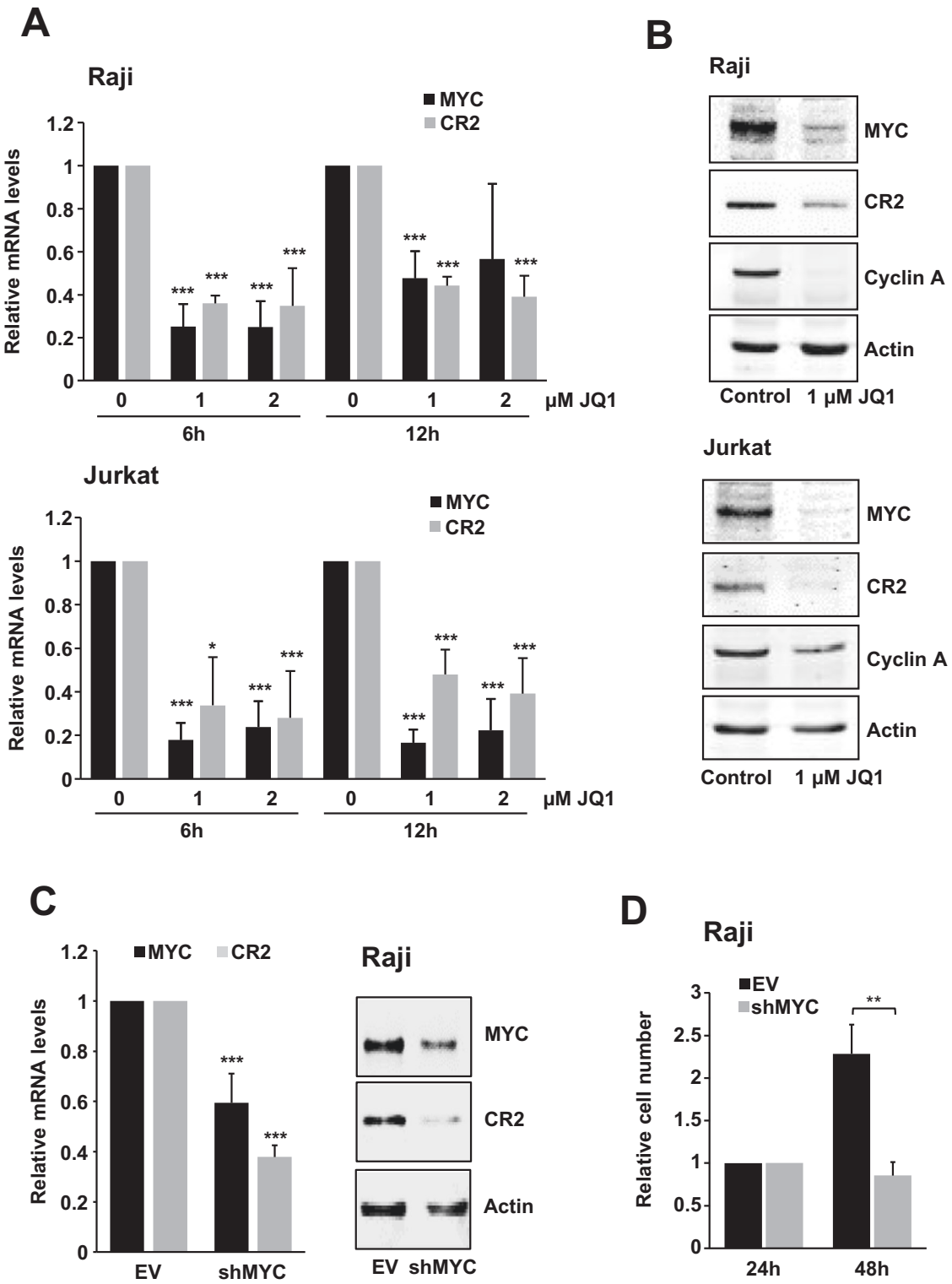

Fig. 1 Downregulation of MYC results in lower CR2 expression. A mRNA expression of *MYC* and *CR2* in Raji and Jurkat cells treated with JQ1 at the indicated concentrations for 6 and 12 h. The expression was determined by RT-qPCR. Data represent mean values ± SD ($n = 3$) *$P < 0.05$; ***$P < 0.005$ (with respect to non-treated cells). **B** Immunoblot showing the protein levels of MYC, CR2 and cyclin A in Raji and Jurkat cells treated with 1 μM JQ1 for 24 h. β-Actin levels were used as loading control. **C** MYC and CR2 mRNA (left panel) and protein (right panel) levels assayed by RT-qPCR and immunoblot, respectively, from Raji cells transduced with either shMYC-containing lentiviral particles or empty vector (EV) control and selected with puromycin. β-Actin levels were used as loading control. Data represent mean values ± SD ($n = 3$). ***$P < 0.005$. **D** Proliferation of Raji cells transduced with either shMYC or EV control lentiviral particles measured by cell count after puromycin selection for 48 h. Data represent mean values ± SD ($n = 3$), normalized to cell counting at the start of the experiment. **$P < 0.01$ by two-tailed unpaired *t*-test.

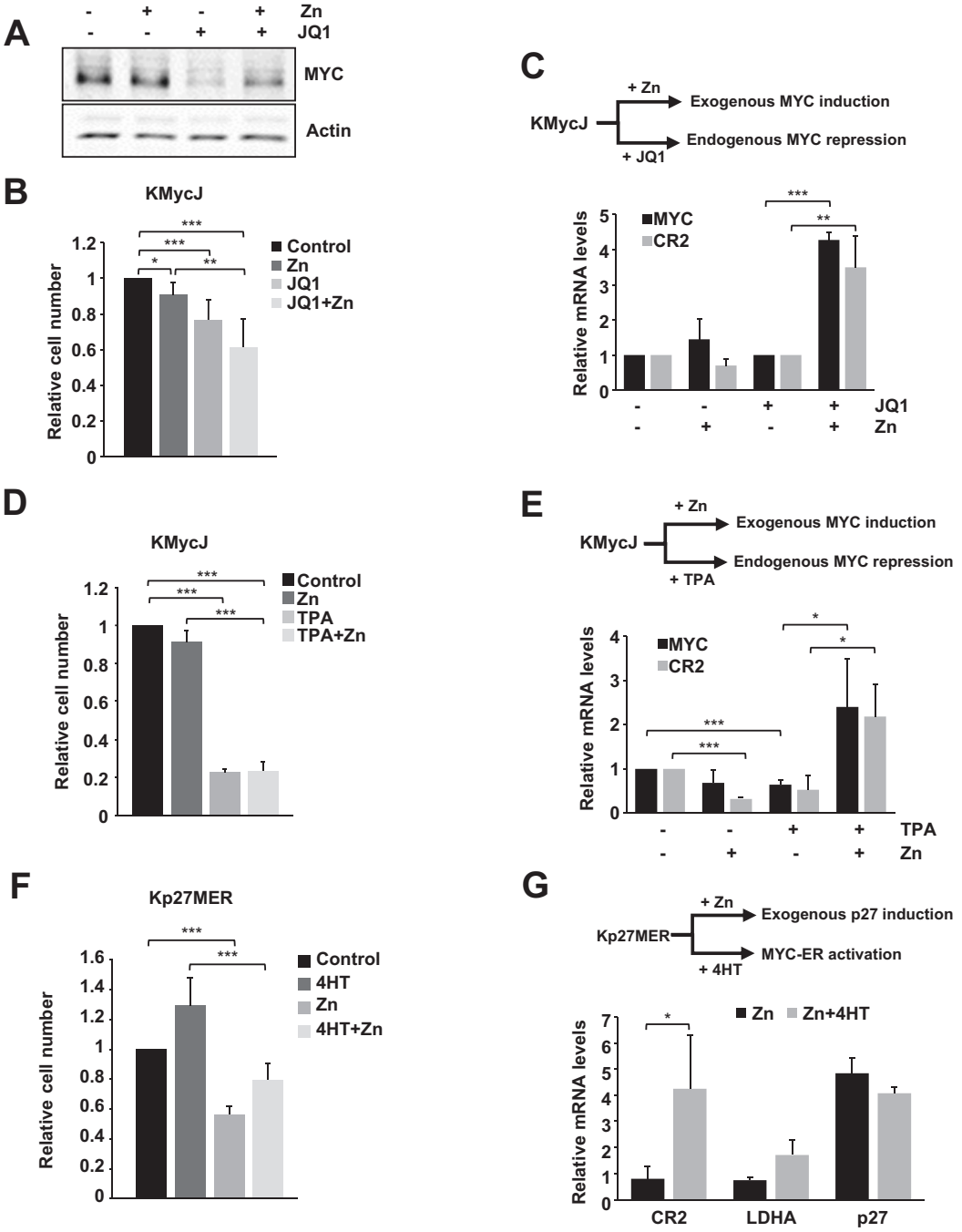

Fig. 2 MYC induces CR2 expression in arrested cells. A Immunoblot showing MYC protein levels of KMycJ cells treated with 75 μM $ZnSO_4$ and 1 μM JQ1 for 24 h. β-Actin levels were used as loading control. **B** Proliferation of KMycJ cells treated with 75 μM $ZnSO_4$ and/or 1 μM JQ1 for 48 h, measured by cell counting and normalized to untreated cells. Data represent mean values ± SD ($n = 4$) *$P < 0.05$; **$P < 0.01$; ***$P < 0.005$. **C** Upper graph: scheme of the conditional MYC expression by $ZnSO_4$ and repression by JQ1 in KMycJ cells. Lower graph: *MYC* and *CR2* mRNA levels in KMycJ cells treated with 75 μM $ZnSO_4$ and/or 1 μM JQ1 for 24 h determined by RT-qPCR. Data represent mean values ± SD ($n = 3$) **$P < 0.01$; ***$P < 0.005$. **D** Proliferation of KMycJ cells treated with 75 μM $ZnSO_4$ and/or 10 nM TPA for 48 h, measured by cell counting and normalized to untreated cells. Data represent mean values ± SD ($n = 3$) ***$P < 0.005$. **E** Upper graph: scheme of the conditional MYC expression by 75 μM $ZnSO_4$ and repression by 10 nM TPA in KMycJ cells. Lower graph: *MYC* and *CR2* expression levels in KMycJ cells treated with $ZnSO_4$ and/or TPA for 48 h determined by RT-qPCR. Data represent mean values ± SD ($n = 3$) *$P < 0.05$; ***$P < 0.005$. **F** Proliferation of Kp27MER cells treated with 200 nM 4HT and/or 75 μM $ZnSO_4$ for 48 h, measured by cell counting and normalized to untreated cells. Data represent mean values ± SD ($n = 4$) **$P < 0.01$; ***$P < 0.005$. **G** Upper graph: scheme of the conditional MYC activation by 4HT and p27 induction by $ZnSO_4$ in Kp27MER cells. Lower graph: *CR2*, *LDHA and p27/CDKN1B* expression from Kp27MER treated with $ZnSO_4$ and 4HT for 24 h determined by RT-qPCR. Data represent mean values ± SD ($n = 3$) *$P < 0.05$ by two-tailed unpaired *t*-test.

in a region 40 bp upstream of the TSS of *CR2* (Fig. 3C). This is consistent with the hypothesis that MYC is a regulator of *CR2* transcription. To validate the MYC-dependent transactivation of *CR2* we performed luciferase assays with a luciferase reporter under the control of the *CR2* promoter region harboring the two E-boxes located ~200 bp upstream the TSS. The reporter was transfected along with a short-hairpin MYC construct. The results showed that knocking down MYC expression leads to a dramatic drop of the *CR2* promoter activity (Fig. 3D). To assess the relevance of the E-boxes for MYC transactivation we carried out ChIP assays on two reporter constructs containing deletions in either E-box 1 or E-box 2. The results showed that the lack of any of the two

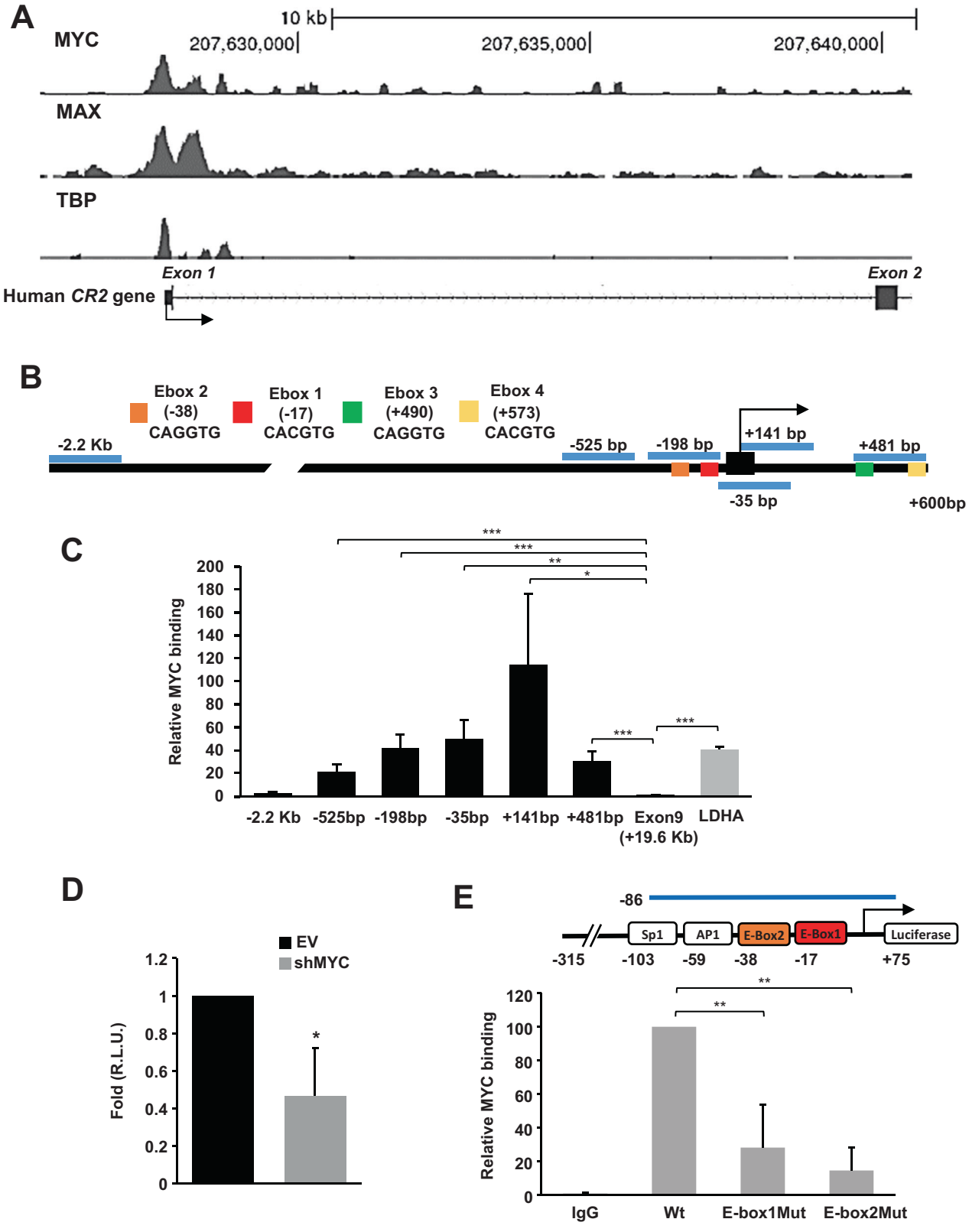

Fig. 3 Binding of MYC to the promoter of *CR2*. **A** Schematic representation of *CR2* chromosome localization and MYC and MAX binding sites according with ChIP-seq data of the ENCODE project (UCSC Genome Browser, GRCh37/hg19 release) in EBV-transformed human B cells (GM12878 cell line). TBP (TATA-box binding protein) is also shown to mark the transcription initiation complex binding. **B** Schematic representation of *CR2* proximal promoter and the first exon and intron. The horizontal bars represent the regions amplified by the different primers used in the ChIP analysis**.** **C** ChIP with anti-MYC antibody on *CR2* gene of Raji cells. Exon9 (+19.6 Kb) of *CR2* gene was used as negative control and an *LDHA* proximal promoter region mapping −85 to +19 bp was used as positive control for MYC binding. Non-specific IgG was used to normalize the data. Data represent mean values ± SD ($n = 3$). *$P < 0.05$; **$P < 0.01$; ***$P < 0.005$ determined by two tail unpaired *t*-test. **D** *CR2* promoter activity measured by luciferase assay of Raji cells transfected with a *CR2* promoter luciferase reporter and transduced with shMYC-containing lentiviral particles (or the corresponding empty vector, EV). Luciferase activity was determined 48 h after infection. Data represent mean values ± SD ($n = 3$). *$P < 0.05$. **E** MYC occupancy on *CR2* promoter assayed by ChIP using an anti-MYC antibody in 293T cells transfected with the luciferase constructs containing either wild-type (Wt) or mutated E-box 1 or E-box 2 *CR2* promoter. The binding of MYC was analyzed on an amplicon (blue line) comprising sequences of *CR2* promoter and of the luciferase ORF. Non-specific IgG was used as negative control and data normalized with respect to the binding of MYC to the wild-type promoter construct. Data represent mean values ± SD ($n = 3$) **$P < 0.01$; ***$P < 0.005$.

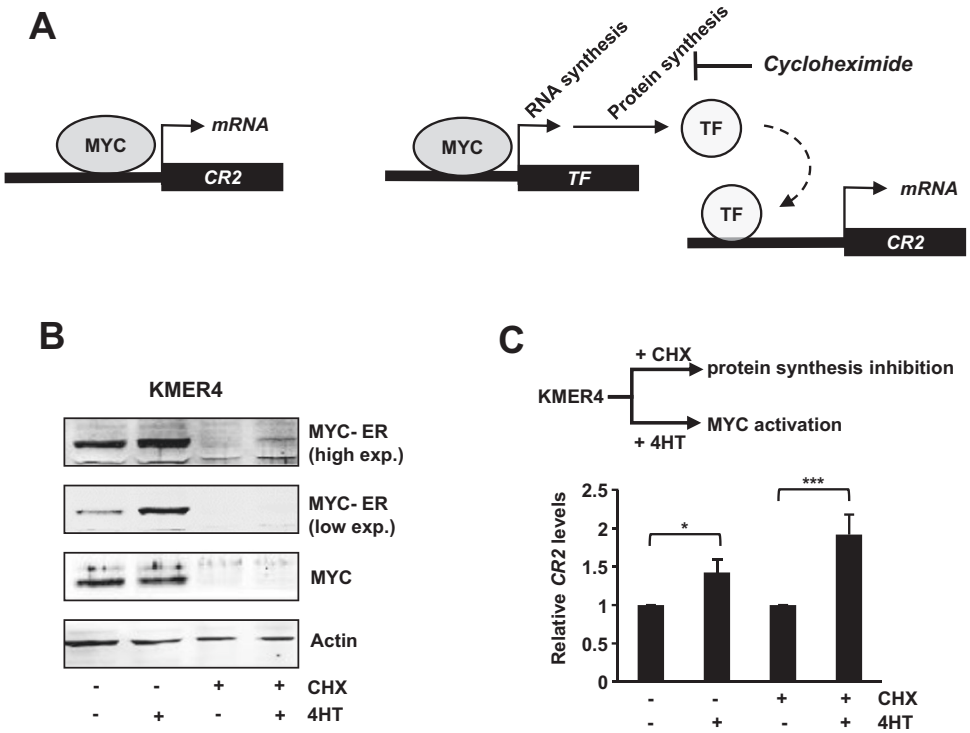

Fig. 4 CR2 is a direct MYC target gene. **A** Scheme showing the two possible mechanisms for MYC-mediated induction of *CR2* expression. Left: the direct cycloheximide insensitive mechanism. Right: the indirect cycloheximide sensitive mechanism by which MYC would induce another transcription factor (TF) which in turn would activate *CR2* expression. **B** MYC and MYC-ER protein levels from KMER4 cells treated with 200 nM 4HT and 50 µg/mL cycloheximide (CHX). After 6 h of treatment, cell lysates were prepared and analyzed by immunoblot. β-Actin levels were used as loading control. **C** Upper graph: scheme of the conditional MYC activation by 4HT and effect of cycloheximide (CHX) in KMER4 cells. Lower graph: expression of *CR2* mRNA in KMER4 cells treated with 4HT and CHX. Data represent mean values ± SD ($n = 3$). *$P < 0.05$; ***$P < 0.005$.

E-boxes significantly decreased MYC occupancy (Fig. 3E). We conclude that MYC binds *CR2* promoter and stimulates its transcription in an E-box-dependent manner.

MYC-ER activation upregulates *CR2* expression in the absence of de novo protein synthesis

Our results showed that MYC induces *CR2* expression independently on MYC-mediated effects on proliferation. However, these results do not rule out the possibility that another MYC target gene encoding for a different transcription factor is responsible for CR2 upregulation. To test whether *CR2* is a direct MYC target, we took advantage of a K562-derived cell line expressing a conditional MYC-Estrogen Receptor chimeric protein (KMER4 cells) which is activatable by 4HT [42]. We asked whether MYC was capable of inducing *CR2* expression in the absence of de novo protein synthesis. We treated KMER4 cells with cycloheximide, a protein synthesis inhibitor, and 4HT. This approach would discriminate between a direct MYC transcripcional effect on *CR2* promoter from an indirect mechanism (Fig. 4A). Endogenous MYC protein levels dramatically decreased after 6 h of cycloheximide treatment, as expected, while MYC-ER was detectable in cells treated with 4HT and cycloheximide (Fig. 4B). Treatment with 4HT, which activated MYC-ER, increased *CR2* mRNA levels even in cycloheximide-treated cells, where new proteins cannot be synthesized. This result rules out the possibility of an intermediate MYC target gene activating *CR2* expression (Fig. 4C). Taken together, the data show that MYC directly activates *CR2* transcription.

Interestingly, CR2 interacts with the BCR complex [46] and is required for optimal B cell proliferation [47, 48]. Thus, we asked whether MYC-mediated upregulation of CR2 could also contribute to B cell proliferation in our model system. To explore this, we silenced *CR2* through lentivirus expressing two short-hairpin

constructs in Raji cells (Supplementary Fig. 3A) and assayed the effect of CR2 depletion on proliferation. The results showed that *CR2* knockdown produced a dramatic decrease in the proliferation of Raji cells (Supplementary Fig. 3B).

MYC induces *CR2* expression in primary B cells

To address whether MYC induces CR2 expression also in primary B cells, we analyzed by flow cytometry the expression of MYC and CR2 in splenic B lymphocytes from C57/BL6 wild-type mice. We found that the fraction of cells with 10% higher MYC expression levels also showed higher CR2 expression (Fig. 5A), thus confirming the correlation observed in human cell lines. A correlation between MYC and CR2 mRNA levels can also be found in hematopoietic human tissues (GEPIA, http://gepia.cancer-pku.cn/) (Supplementary Fig. 4). To confirm this correlation we analyzed Cr2 expression in mice where *Myc* can be conditionally depleted in primary B lymphocytes in the $Myc^{fl/fl}$;$Max^{fl/+}$;$Cd19^{cre/+}$;$Rosa26^{gfp/gfp}$ (MycKO-Cd19) model previously described by us [49]. This mouse carries one allele of *Max* and both alleles of *Myc* flanked by *loxp* sites. Expression of *Cre* recombinase is driven by the endogenous promoter of *Cd19* and promotes specific *Myc* deletion in B lymphocytes and expression of GFP [49]. GFP allows the rapid identification and analysis of B lymphocytes that have undergone deletion of *Myc*. Primary B lymphocytes from the spleens of MycKO-Cd19 and heterozygous control mice were activated with LPS and interleukin-4, stained with anti-Cr2/Cd21 antibody and analyzed by flow cytometry. We observed a dramatic decrease in the population of $Cr2/Cd21^{+}$ cells within the GFP^{+} population (*Myc* deleted cells) in the MycKO-Cd19 compared to heterozygous control mice before and after 48 h of activation (Fig. 5B). To see whether this effect was specific for *Cr2/Cd21*, we analyzed the surface expression of the activation marker CD69 on the same cells. We did not see any significant differences in CD69 surface expression between mutant and control cells (Supplementary Fig. 5). To confirm the induction of *Cr2* by Myc, we overexpressed MYC in primary mouse splenic B cells by retroviral transduction with MYC, encoded in an Orange-reporter bicistronic IRES vector (Fig. 5C), as well as with control Orange retrovirus. We found that MYC-transduced cells expressed higher *Cr2* levels (Fig. 5C). In light of these data, we conclude that MYC promotes CR2 expression not only in human cell lines but also in murine primary B cells.

MYC depletion decreases and MYC expression enhances EBV infection efficiency

Our results indicate that the EBV receptor, CR2, is a direct MYC target gene. Thus, we wanted to elucidate whether the modulation of MYC expression correlated with the infection capacity of EBV. Unlike Raji cells, Ramos is an EBV-negative BL cell line and thus a suitable model to test this hypothesis, despite the low CR2 expression in these cells. We first confirmed that, in contrast to Raji cells, total genomic DNA (gDNA) of Ramos did not contain EBV sequences (Fig. 6A). We then confirmed by immunoblot the downregulation of MYC protein upon shMYC lentiviral infection of Ramos cells. Both shMYC lentiviral constructs were able to silence MYC in Ramos cells (Fig. 6B) and we used a mix of both shMYC virus in subsequent experiments. Transduction of Ramos cells with shMYC resulted in downregulation of *MYC* and *CR2* mRNA (Fig. 6C). To investigate the correlation between MYC and EBV infection, cells were transduced with shMYC lentivirus, selected with puromycin and infected with EBV-containing supernatants from a producer cell line (Fig. 6D). gDNA was prepared from control and MYC-depleted Ramos cells and sequences of *EBNA1* and *LMP1* were measured to quantify EBV infection by qPCR. Cells previously infected with shMYC lentivirus showed reduced content of EBV genes (Fig. 6E). These results cannot be explained by a slower growth of MYC-silenced cells as the proliferation rate of the cells did not significantly modify the extent of EBV infection (Supplementary Fig. 6). We sought to confirm these results through a complementary approach, testing the infection of EBV by the presence of a viral protein (gp350/250) in the cells membrane after short exposure to the virus. Raji cells were used as they express higher CR2 levels than Ramos. Cells were transduced with shMYC lentivirus, selected with puromycin and infected with EBV for 2.5 h (Fig. 6F). Silencing of MYC was assessed by RT-qPCR (Fig. 6G). The quantification of the immunofluorescence analyses showed that in cells with lower MYC expression, the level of EBV infection dropped significantly (Fig. 6H). As JQ1 downregulates MYC in Raji cells (Fig. 1), we also tested the extent of EBV infection in cells treated with JQ1. The result showed a dramatic decrease in the fraction of EBV-infected cells as assessed by immunofluorescence (Supplementary Fig. 7). The decrease of MYC at the protein level was also confirmed by double immunofluorescence in cells either transduced with shMYC lentivirus or treated with JQ1 (Supplementary Fig. 8).

In a second experimental approach, we overexpressed MYC by transducing Ramos cells with a lentiviral vector that expressed MYC (LvMYC). Three days after lentiviral infection and puromycin selection, cells were infected with EBV for a further 48 h (Fig. 7A). The protein levels of MYC in transduced cells were confirmed by immunoblot (Fig. 7B). Total gDNA was prepared and the levels of *EBNA1* and *LMP1* DNA were analyzed by qPCR. The results showed an increased infection in cells expressing higher MYC levels (Fig. 7C). Altogether, the results indicate that EBV infection is enhanced by high MYC levels.

DISCUSSION

In this work, we propose a new mechanism for the pathogenesis of BL, based on the MYC-mediated induction of CR2, the EBV receptor. We found a *CR2* downregulation in B and T cell lines (Raji and Jurkat cell lines, respectively) treated with the drug JQ1, described as a potent inhibitor of MYC expression, and with short hairpin (sh) constructs of MYC. These results, together with our initial observation in K562 cells, confirmed that MYC regulates *CR2* expression, a result also observed in transcriptomic studies in different cell lines including B cells [6, 50, 51]. Both JQ1 and shMYC caused proliferation arrest, mediated by low MYC levels. Therefore, it was conceivable that CR2 downregulation could be a consequence of the proliferation arrest instead of being directly transactivated by MYC. The same effect may apply to other MYC-regulated genes revealed in transcriptomic studies. To analyze MYC-mediated induction of CR2 in the absence of cell proliferation, we used cells engineered with inducible MYC alleles and observed *CR2* upregulation in response to MYC expression in arrested cells upon JQ1 treatment. Noteworthy, JQ1 and other BET inhibitors are currently being tested in clinical trials in B cell malignancies primarily due to their effect on MYC expression [39]. However, our results show that ectopic MYC expression fails to rescue the anti-proliferative effect of JQ1, suggesting that the anti-tumoral effect of the BRD4 inhibitor is not only dependent on MYC repression. Additionally, we used two other experimental approaches in which MYC activity can be induced upon arrested proliferation, i.e., by TPA treatment and by p27 enforced expression. Both proved that MYC-dependent *CR2* induction is not a consequence of MYC-induced proliferation but a direct effect of MYC. These studies were performed in human cell lines; however, using mice with a Myc-conditional knock-out allele and mouse primary B cells transduced with MYC we showed that MYC-mediated upregulation of *Cr2* gene in murine primary B cells.

These results showed that *CR2* upregulation after MYC overexpression (and *CR2* downregulation after MYC depletion) is independent of the proliferative state of the cells, consistently with *CR2* being a direct MYC target gene. To further confirm this,

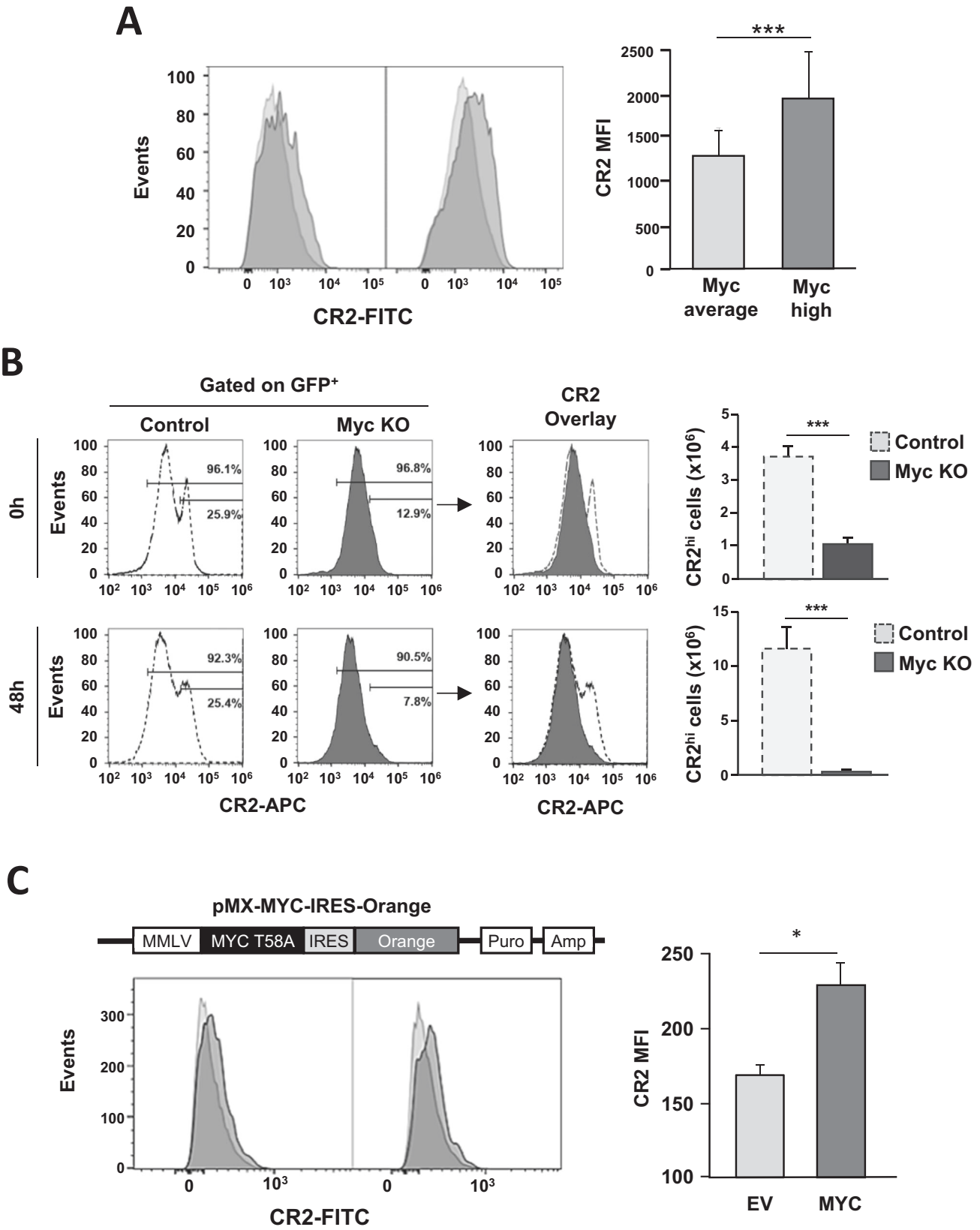

we performed (i) ChIP experiments showing MYC binding close to the human *CR2* TSS, which required the presence of two E-boxes and (ii) luciferase reporter assays showing that MYC activated the *CR2* promoter. These results suggested that *CR2* is a MYC direct target gene. Nonetheless, two facts must be noted: first, binding to chromatin does not mean that a gene is actually transactivated by a transcription factor, and second, that there are many transcription factors that are themselves MYC target genes. Thus,

Fig. 5 Myc induces *CR2* expression in primary B cells. A Cell surface CR2/CD21 levels in splenic mouse B cells with the 10% highest MYC expression levels (dark gray) as compared to the rest of the cells (light gray). B cells were prepared from 18-week-old C57/BL6 wild-type mice analyzed by flow cytometry. Two representative overlay histograms are shown on the left and quantification of CR2 mean fluorescence intensity (MFI) at the right. Data are mean values ± SD ($n = 6$) ***$P < 0.005$. **B** Mature B lymphocytes from the spleens of $Myc^{flox/flox}$;$Max^{flox/+}$;$cd19^{cre/+}$;$Rosa26^{gfp/gfp}$ (MycKO, $n = 3$) homozygous and $Myc^{flox/+}$;$Max^{flox/+}$;$Cd19^{cre/+}$;$Rosa26^{gfp/gfp}$ heterozygous control ($n = 3$) mice were activated with LPS and IL4 for 48 h. Cells were stained with the indicated antibodies and analyzed by flow cytometry. GFP^+ cells (*Myc* deleted B lymphocytes) were gated and surface expression of CR2/CD21 was analyzed. Absolute numbers of $CR2^{hi}$ are shown. $n = 3$, ***$P < 0.005$. by two-tailed unpaired *t*-test**. C** Left panel, upper graph: schematic representation of the pMX-MYC-IRES-Orange retroviral vector used in the experiments. MMLV: LTR and ψ sequences of MMLV virus; Puro and Amp, puromycin and ampicillin resistance genes. Right panel, bottom graph: expression of CR2 in mouse splenic B cells after MYC overexpression. $CD43^-$ B cells isolated from spleens were cultured with LPS and interleukin-4 for 24 h and transduced with pMX-MYC-Orange retrovirus and the control retrovirus (EV) during 48 h. CR2 was assayed in Orange+ transduced cells. Two representative overlay histograms are shown at the left and quantification of CR2 mean fluorescence intensity (MFI) at the right. Data are mean values ± SD, $n = 5$, *$P < 0.05$ by two-tailed unpaired *t*-test.

it is possible that MYC induces other transcription factor(s), which in turn induces *CR2*. However, we ruled out this possibility as MYC was able to activate *CR2* transcription in the absence of de novo protein synthesis. Thus, we conclude that *CR2* is a direct MYC target gene. The analysis of the expression data from 60 BL available in public databases shows that there is not a tight correlation between MYC and CR2 levels, although MYC missense mutations are significantly more frequent in lymphomas with higher CR2 expression (cBioPortal, http://cbioportal.org) [52]. It is possible that *CR2* upregulation by MYC occurs at the first stages of cell transformation into BL cell and is not maintained through subsequent advanced stages. It must also be noted that MYC expression is already high in the advanced lymphomas included in these transcriptomic studies, so a lack of correlation would not be surprising since there are no low MYC-expressing samples to compare with. Finally, there are other transcription factors known to regulate *CR2* expression acting on the promoter (e.g., AP1, USF1, SP1, NFκB and NOTCH1) that may operate in advanced but not early tumor stages [53–56], two of them (NOTCH1 and NFκB) reported to be positive regulators of MYC transcription in lymphoid cells [57, 58].

The relationship between EBV infection and MYC translocation events in BL is a matter of debate as the mechanism whereby EBV leads to MYC dysregulation remains ill-defined. The most accepted hypothesis proposes that EBV infection would lead to the activation and expansion of germinal center B cells and subsequent MYC translocation (schematized in Fig. 8). Indeed, the correlation between high EBV antibody titers and BL found in African children led to declare EBV as the causative agent of BL [33]. However, other evidence argue against this "virus first" model. First, in most sBL cases EBV infection is absent, while *MYC* is translocated in all cases. Moreover, although there are differences in the prevalence of some genetic alterations and gene expression pattern, there are no differential molecular markers in the mutational landscape between EBV^+ and EBV^- lymphomas, including mutations in the *MYC* gene [15, 21, 59–61]. Second, more than 95% of the human adult population has been infected by EBV, but oncogenic events related to EBV infection have a very low incidence, and actually, the prevalence of EBV-positive BL is decreasing [24]. Third, *MYC* translocation is not found in other tumors associated with EBV infection, remarkably nasopharyngeal cancer, gastric cancer and Hodgkin lymphoma [62–64]. Fourth, the EBV genes required for B cell transformation into lymphoblastoid cell lines are not expressed in BL. Indeed, only the latent EBNA1 protein is consistently expressed in BL and is unable to transform B cells. Moreover, MYC represses the EBV-transforming LMP1 gene [65]. It has been reported that EBNA2 and EBNA3C induce MYC expression [66–68], and that EBNA3C induces AID, which could generate chromosomal translocations involving MYC [18, 19, 69]. EBV could induce other genetic changes in EBV-infected B cells [61]. However, neither EBNA2 nor EBNA3C are expressed in BL.

Here we have shown that *CR2* is a MYC target gene and that *MYC* knockdown results in decreased EBV infection, whereas *MYC* overexpression results in increased infection. A limitation of our study is that our data are generated with human BL cell lines, not primary human B cells. However, it is tempting to speculate that, at least in a relevant fraction of eBL cases, *MYC* dysregulation occurs first, facilitating subsequent EBV infection. It must be noted that our results do not contradict the canonical hypothesis ("virus first") for BL development. Rather, they are consistent with an alternative (but not mutually exclusive), "MYC first" mechanism that would be at least partially responsible for the correlation between eBL and EBV infection. Both hypotheses are depicted in Fig. 8. In accordance with the "MYC first" hypothesis, those B cells with high MYC levels (due to translocation) would show an increased density of CR2 receptors, thus augmenting the probability of EBV infection. In agreement with previous reports [40] we have detected in our Raji model that MYC knockdown activates EBV lytic genes. Therefore, MYC would enhance viral infection on the one hand but prevent the lytic cycle of infected cells on the other hand. The "MYC first" mechanism would be compatible with the epidemiological data and the viral clonality data, as the subsequent EBV infection will co-adjuvate to lymphoma development through demonstrated mechanisms such as inhibition of apoptosis and evasion of the immune surveillance, thus favoring the selection of MYC-expressing and EBV-infected cell clones. In conclusion, our results showing that *CR2* is a direct MYC target gene provide new insights into the understanding of BL. Further research should be undertaken to investigate the potential of *CR2* regulation by MYC as a new therapeutic approach for BL treatment.

METHODS

Extended methods are included in the Supplementary Information

Cell culture and proliferation

Raji, Jurkat, Ramos, K562, KMycJ, KMER4, Kp27MER and B95-8 were grown in RPMI-1640 and HeLa, HEK293T in DMEM both with 10% FBS and antibiotics. Viable cells were counted in hemocytometer with Trypan Blue or in a Guava cell counter (Millipore).

Cell cycle and apoptosis

For cell cycle, cells were washed once with PBS, stained with Hoechst and analyzed by flow cytometry. Apoptosis was assayed with the Annexin V-PE apoptosis detection kit (Immunostep).

RNA and DNA extraction and quantification

RNA extraction was performed using TriReagent (Sigma-Aldrich). Reverse transcription was performed using the iScript cDNA Synthesis Kit (Bio-Rad). For EBV lytic genes, RNAs were treated with DNase I (Invitrogen) prior to cDNA synthesis. gDNA was extracted with Qiagen DNeasy Blood & Tissue kit. qPCRs were performed using 2xSYBR Select Master mix (Applied Biosystem).

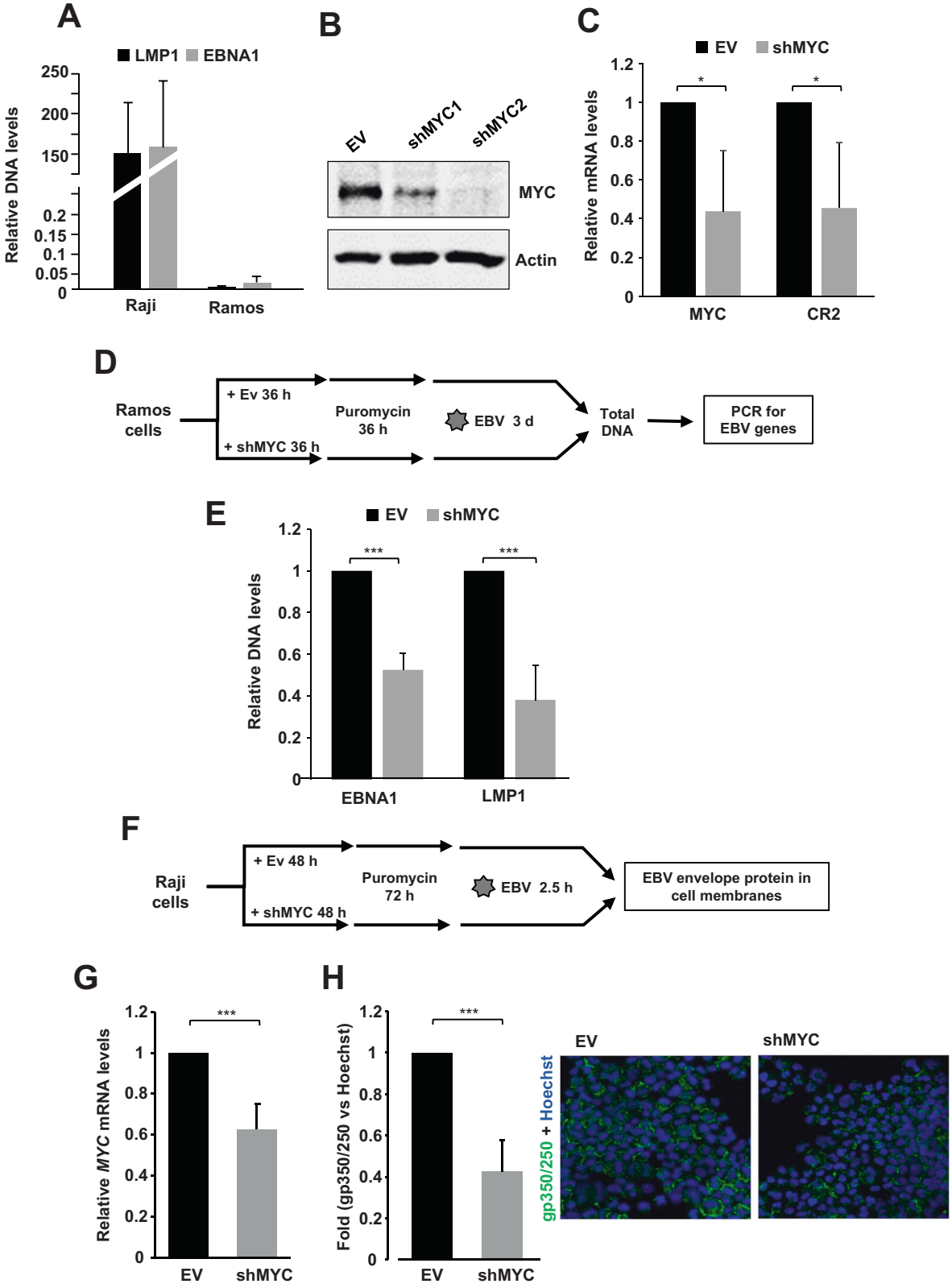

Immunoblots

Cells were lysed in 1% NP40 lysis buffer [70]. Protein extracts were sonicated and further clarified by centrifugation. Samples were resolved by SDS-PAGE and transferred to a nitrocellulose membrane. Signals were recorded with an Odyssey Infrared Imaging Scanner (LiCor Biosciences).

Transfection and luciferase assays

Luciferase vectors were transfected using Amaxa Nucleofector for Raji and K562 cells. HEK293T cells were transfected using PEI (Polysciences, Inc). Dual-Luciferase Reporter Assay System (Promega) was used.

Fig. 6 MYC depletion decreases EBV infection of B cells. A gDNA levels of *LMP1* and *EBNA1* viral genes from Raji and Ramos cells analyzed by PCR. Data normalized against *LDHA* and *CR2* gDNA levels (same genomic regions used in ChIP experiments (Supplementary Table 1). **B** Depletion of MYC protein assessed by immunoblot after lentiviral transduction with two short-hairpin MYC constructs in Ramos cells. Subsequent experiments were performed using a mixture of the two shRNA. **C** *MYC* and *CR2* mRNA levels from Ramos cells transduced with lentiviral particles expressing shMYC and empty vector (EV) followed by 3 days of EBV infection and analyzed by RT-qPCR. Data represent mean values ± SD ($n = 3$). *$P < 0.05$. **D** Scheme of the experiment. **E** *EBNA1 and LMP1* gDNA levels in Ramos cells infected with EBV, quantified by qPCR. Data represent mean values ± SD ($n = 3$) ***$P < 0.005$**. F** Scheme of the experiment**. G** *MYC* mRNA levels from Raji cells transduced with lentiviral particles expressing shMYC or empty vector (EV), analyzed by RT-qPCR after 3 days of puromycin selection. Data represent mean values ± SD ($n = 3$). ***$P < 0.005$. **H** Levels of the EBV envelope protein gp350/250 in control cells (EV) and MYC knockdown (shMYC) cells after 2.5 h of EBV infection. The gp350/250 area was normalized to the nuclei area. Data represent mean values ± SD ($n = 3$) ***$P < 0.05$. Right panel: representative field showing the gp350/250 (green) and nuclei stained with Hoechst 33342 (blue).

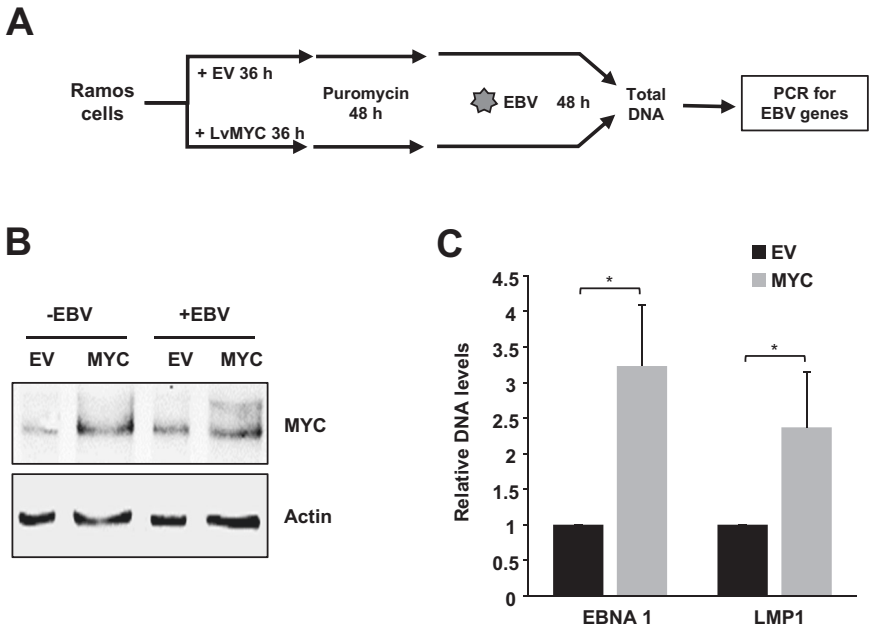

Fig. 7 MYC overexpression increases EBV infection of B cells. A Scheme of the experiment. **B** Immunoblot showing the levels of MYC in cells transduced with lentivirus expressing MYC and the empty vector (EV) followed by 48 h of EBV infection. β-Actin was used as loading control. **C** *EBNA1 and LMP1* gDNA levels in Ramos cells transduced with MYC lentivirus and EBV, quantified by RT-qPCR. Data represent mean values ± SD ($n = 3$). *$P < 0.05$.

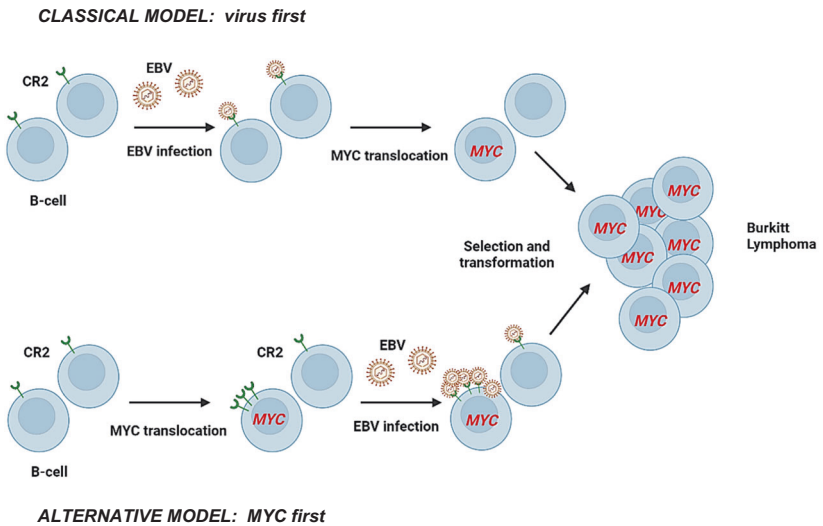

Fig. 8 Two non-mutually exclusive models for pathogenesis of Burkitt lymphoma. In the "classical" model, EBV infection occurs first and promotes MYC translocation. The results presented here allow the proposal of a second model by which MYC translocation in tumor-initiating cells leads to overexpression of CR2, thus facilitating EBV infection. Created with BioRender.com.

Retroviral constructs
The AID sequences were removed from the pMXPIE-AID retroviral vector [71] and the resulting backbone was linked to the orange fluorescent protein gene mOrange2 generating the empty plasmid pMX-IRES-mOrange2 further used to generate a pMX-MYC-IRES-mOrange2.

Lentivirus and retrovirus production
For lentivirus production, HEK293T cells were transfected with PEI with the lentiviral packaging plasmids and the construct of interest. Supernatants were concentrated with PEG8000. Retroviral supernatants were produced by transient calcium phosphate transfection of NIH-293T cells with pCL-ECO (Novus) and pMX-Orange or pMX-MYC-Orange retroviral constructs.

Flow cytometry and retroviral infection of mouse primary B cells
Single-cell suspensions from spleens were placed in culture and the mature B lymphocytes were activated with LPS and IL4, and stained with antibodies. Mouse primary B cells were purified from spleens of 4-month-old C57/BL6 mice by anti-CD43, cultured for 24 h and transduced with control pMX-Orange or pMX-MYC-Orange retrovirus. CD21 expression was analyzed by flow cytometry in Orange-positive transduced cells.

Chromatin immunoprecipitation
Cells were fixed with 1% formaldehyde. After lysis, chromatin was sheared to 1000–500 bp fragments using a Bioruptor Plus Sonicator; 2–3 µg of antibody were added to diluted extracts and incubated at 4 °C overnight rotating. Immunoprecipitated material was purified with Dynabeads Protein G (Invitrogen). Samples were eluted and des-crosslinked. DNA was purified with Qiaquick PCR purification kit (Qiagen).

Immunofluorescence
Slides of Raji cells were obtained using a Cytospin, fixed with 4% PFA and blocked with 1% BSA-PBS. For double immunofluorescence, samples were permeabilized with Triton X-100 before blocking. Primary antibodies were incubated for 2 h, RT, washed with PBS and incubated with secondary antibodies for 1 h at RT. Hoechst 3342 was used to stain nuclei. ImageJ software was used for analysis and quantification.

EBV production
B95-8 cells were grown to saturation in 20% FBS-RPMI. After 3 weeks, EBV-containing supernatants were collected and stored at −80 °C. For short-term infections, EBV was concentrated (20×) with 10% PEG8000.

Statistical analyses
Significance was determined by Student's two-tailed one-sample *t*-test unless otherwise specified. The Shapiro–Wilk normality test was applied to check normal distributions.

DATA AVAILABILITY
The authors declare that all data that support the findings of this study are available within the paper and supplementary files.

REFERENCES
1. Dang CV. MYC on the path to cancer. Cell. 2012;149:22–35.
2. Conacci-Sorrell M, McFerrin L, Eisenman RN. An overview of MYC and its interactome. Cold Spring Harb Perspect Med. 2014;4:1–24.
3. Bretones G, Delgado MD, Leon J. Myc and cell cycle control. Biochim Biophys Acta. 2015;1849:506–16.
4. Zeller KI, Zhao X, Lee CW, Chiu KP, Yao F, Yustein JT, et al. Global mapping of c-Myc binding sites and target gene networks in human B cells. Proc Natl Acad Sci USA. 2006;103:17834–9.
5. Sabo A, Kress TR, Pelizzola M, de Pretis S, Gorski MM, Tesi A, et al. Selective transcriptional regulation by Myc in cellular growth control and lymphomagenesis. Nature. 2014;511:488–92.
6. Nie Z, Hu G, Wei G, Cui K, Yamane A, Resch W, et al. c-Myc is a universal amplifier of expressed genes in lymphocytes and embryonic stem cells. Cell. 2012;151:68–79.
7. Lin CY, Loven J, Rahl PB, Paranal RM, Burge CB, Bradner JE, et al. Transcriptional amplification in tumor cells with elevated c-Myc. Cell. 2012;151:56–67.
8. Kress TR, Sabò A, Amati B. MYC: connecting selective transcriptional control to global RNA production. Nat Rev Cancer. 2015;15:593–607.
9. Kalkat M, De Melo J, Hickman KA, Lourenco C, Redel C, Resetca D, et al. MYC deregulation in primary human cancers. Genes (Basel). 2017;8:151.
10. Schaub FX, Dhankani V, Berger AC, Trivedi M, Richardson AB, Shaw R, et al. Pan-cancer alterations of the MYC oncogene and its proximal network across the Cancer Genome Atlas. Cell Syst. 2018;6:282–300.e2.
11. Delgado MD, Leon J. Myc roles in hematopoiesis and leukemia. Genes Cancer. 2010;1:605–16.
12. Ott G, Rosenwald A, Campo E. Understanding MYC-driven aggressive B-cell lymphomas: pathogenesis and classification. Blood. 2013;122:3884–91.
13. Burkitt D. A sarcoma involving the jaws in African children. Br J Surg. 1958;46:218–23.
14. Molyneux EM, Rochford R, Griffin B, Newton R, Jackson G, Menon G, et al. Burkitt's lymphoma. Lancet. 2012;379:1234–44.
15. Schmitz R, Young RM, Ceribelli M, Jhavar S, Xiao W, Zhang M, et al. Burkitt lymphoma pathogenesis and therapeutic targets from structural and functional genomics. Nature. 2012;490:116–20.
16. Bisso A, Sabò A, Amati B. MYC in Germinal Center-derived lymphomas: mechanisms and therapeutic opportunities. Immunol Rev. 2019;288:178–97.
17. Methot SP, Di Noia JM. Molecular mechanisms of somatic hypermutation and class switch recombination. Adv Immunol. 2017;133:37–87.
18. Ramiro AR, Jankovic M, Eisenreich T, Difilippantonio S, Chen-Kiang S, Muramatsu M, et al. AID is required for c-myc/IgH chromosome translocations in vivo. Cell. 2004;118:431–8.
19. Robbiani DF, Bothmer A, Callen E, Reina-San-Martin B, Dorsett Y, Difilippantonio S, et al. AID is required for the chromosomal breaks in c-myc that lead to c-myc/IgH translocations. Cell. 2008;135:1028–38.
20. Bhatia K, Huppi K, Spangler G, Siwarski D, Iyer R, Magrath I. Point mutations in the c-Myc transactivation domain are common in Burkitt's lymphoma and mouse plasmacytomas. Nat Genet. 1993;5:56–61.
21. Lopez C, Kleinheinz K, Aukema SM, Rohde M, Bernhart SH, Hubschmann D, et al. Genomic and transcriptomic changes complement each other in the pathogenesis of sporadic Burkitt lymphoma. Nat Commun. 2019;10:1459.
22. Farrell AS, Sears RC. MYC degradation. Cold Spring Harb Perspect Med. 2014;4:a014365.
23. Thorley-Lawson DA, Allday MJ. The curious case of the tumour virus: 50 years of Burkitt's lymphoma. Nat Rev Microbiol. 2008;6:913–24.
24. Al-Khreisat MJ, Ismail NH, Tabnjh A, Hussain FA, Mohamed Yusoff AA, Johan MF, et al. Worldwide prevalence of Epstein-Barr virus in patients with Burkitt lymphoma: a systematic review and meta-analysis. Diagnostics (Basel). 2023;13:2068.
25. Dunmire SK, Verghese PS, Balfour HH Jr. Primary Epstein-Barr virus infection. J Clin Virol. 2018;102:84–92.
26. Young LS, Yap LF, Murray PG. Epstein-Barr virus: more than 50 years old and still providing surprises. Nat Rev Cancer. 2016;16:789–802.
27. Soldan SS, Lieberman PM. Epstein-Barr virus and multiple sclerosis. Nat Rev Microbiol. 2023;21:51–64.
28. Rowe M, Kelly GL, Bell AI, Rickinson AB. Burkitt's lymphoma: the Rosetta Stone deciphering Epstein-Barr virus biology. Semin Cancer Biol. 2009;19:377–88.
29. Mancao C, Hammerschmidt W. Epstein-Barr virus latent membrane protein 2A is a B-cell receptor mimic and essential for B-cell survival. Blood. 2007;110:3715–21.
30. Kelly GL, Milner AE, Tierney RJ, Croom-Carter DS, Altmann M, Hammerschmidt W, et al. Epstein-Barr virus nuclear antigen 2 (EBNA2) gene deletion is consistently linked with EBNA3A, -3B, and -3C expression in Burkitt's lymphoma cells and with increased resistance to apoptosis. J Virol. 2005;79:10709–17.
31. Wang LW, Shen H, Nobre L, Ersing I, Paulo JA, Trudeau S, et al. Epstein-Barr-virus-induced one-carbon metabolism drives B cell transformation. Cell Metab. 2019;30:539–55.e11.
32. Geser A, de The G, Lenoir G, Day NE, Williams EH. Final case reporting from the Ugandan prospective study of the relationship between EBV and Burkitt's lymphoma. Int J Cancer. 1982;29:397–400.
33. IARC. Biological Agentes. A review of human carcinogenesis. Epstein-Barr virus. IARC Monographs. 2012;100B:49–92.
34. Sugden B. Epstein-Barr virus: the path from association to causality for a ubiquitous human pathogen. PLoS Biol. 2014;12:e1001939.
35. López C, Burkhardt B, Chan JKC, Leoncini L, Mbulaiteye SM, Ogwang MD, et al. Burkitt lymphoma. Nat Rev Dis Primers. 2022;8:78.
36. Allday MJ. How does Epstein-Barr virus (EBV) complement the activation of Myc in the pathogenesis of Burkitt's lymphoma? Semin Cancer Biol. 2009;19:366–76.
37. Nemerow GR, Wolfert R, McNaughton ME, Cooper NR. Identification and characterization of the Epstein-Barr virus receptor on human B lymphocytes and its relationship to the C3d complement receptor (CR2). J Virol. 1985;55:347–51.
38. Fearon DT, Carter RH. The CD19/CR2/TAPA-1 complex of B lymphocytes: linking natural to acquired immunity. Annu Rev Immunol. 1995;13:127–49.

39. Mertz JA, Conery AR, Bryant BM, Sandy P, Balasubramanian S, Mele DA, et al. Targeting MYC dependence in cancer by inhibiting BET bromodomains. Proc Natl Acad Sci USA. 2011;108:16669–74.
40. Guo R, Jiang C, Zhang Y, Govande A, Trudeau SJ, Chen F, et al. MYC controls the Epstein-Barr virus lytic switch. Mol Cell. 2020;78:653–69.e8.
41. Gargouri B, Van Pelt J, El Feki Ael F, Attia H, Lassoued S. Induction of Epstein-Barr virus (EBV) lytic cycle in vitro causes oxidative stress in lymphoblastoid B cell lines. Mol Cell Biochem. 2009;324:55–63.
42. Acosta JC, Ferrandiz N, Bretones G, Torrano V, Blanco R, Richard C, et al. Myc inhibits p27-induced erythroid differentiation of leukemia cells by repressing erythroid master genes without reversing p27-mediated cell cycle arrest. Mol Cell Biol. 2008;28:7286–95.
43. Penn LJ, Brooks MW, Laufer EM, Land H. Negative autoregulation of c-myc transcription. Embo J. 1990;9:1113–21.
44. Delgado MD, Lerga A, Canelles M, Gomez-Casares MT, Leon J. Differential regulation of Max and role of c-Myc during erythroid and myelomonocytic differentiation of K562 cells. Oncogene. 1995;10:1659–65.
45. Shim H, Dolde C, Lewis BC, Wu CS, Dang G, Jungmann RA, et al. c-Myc transactivation of LDH-A: implications for tumor metabolism and growth. Proc Natl Acad Sci USA. 1997;94:6658–63.
46. Schweighoffer E, Tybulewicz VL. Signalling for B cell survival. Curr Opin Cell Biol. 2018;51:8–14.
47. Ahearn JM, Fischer MB, Croix D, Goerg S, Ma M, Xia J, et al. Disruption of the Cr2 locus results in a reduction in B-1a cells and in an impaired B cell response to T-dependent antigen. Immunity. 1996;4:251–62.
48. Cherukuri A, Cheng PC, Pierce SK. The role of the CD19/CD21 complex in B cell processing and presentation of complement-tagged antigens. J Immunol. 2001;167:163–72.
49. Perez-Olivares M, Trento A, Rodriguez-Acebes S, Gonzalez-Acosta D, Fernandez-Antoran D, Roman-Garcia S, et al. Functional interplay between c-Myc and Max in B lymphocyte differentiation. EMBO Rep. 2018;19:e45770.
50. Fernandez PC, Frank SR, Wang L, Schroeder M, Liu S, Greene J, et al. Genomic targets of the human c-Myc protein. Genes Dev. 2003;17:1115–29.
51. Li Z, Van Calcar S, Qu C, Cavenee WK, Zhang MQ, Ren B. A global transcriptional regulatory role for c-Myc in Burkitt's lymphoma cells. Proc Natl Acad Sci USA. 2003;100:8164–9.
52. Cerami E, Gao J, Dogrusoz U, Gross BE, Sumer SO, Aksoy BA, et al. The cBio cancer genomics portal: an open platform for exploring multidimensional cancer genomics data. Cancer Discov. 2012;2:401–4.
53. Vereshchagina LA, Tolnay M, Tsokos GC. Multiple transcription factors regulate the inducible expression of the human complement receptor 2 promoter. J Immunol. 2001;166:6156–63.
54. Ng HL, Taylor RL, Cheng J, Abraham LJ, Quail E, Cruickshank MN, et al. Notch signaling induces a transcriptionally permissive state at the Complement C3d Receptor 2 (CR2) promoter in a pre-B cell model. Mol Immunol. 2020;128:150–64.
55. Ulgiati D, Pham C, Holers VM. Functional analysis of the human complement receptor 2 (CR2/CD21) promoter: characterization of basal transcriptional mechanisms. J Immunol. 2002;168:6279–85.
56. Tolnay M, Vereshchagina LA, Tsokos GC. NF-kappaB regulates the expression of the human complement receptor 2 gene. J Immunol. 2002;169:6236–43.
57. Kanda K, Hu HM, Zhang L, Grandchamps J, Boxer LM. NF-kappa B activity is required for the deregulation of c-myc expression by the immunoglobulin heavy chain enhancer. J Biol Chem. 2000;275:32338–46.
58. Weng AP, Millholland JM, Yashiro-Ohtani Y, Arcangeli ML, Lau A, Wai C, et al. c-Myc is an important direct target of Notch1 in T-cell acute lymphoblastic leukemia/lymphoma. Genes Dev. 2006;20:2096–109.
59. Abate F, Ambrosio MR, Mundo L, Laginestra MA, Fuligni F, Rossi M, et al. Distinct viral and mutational spectrum of endemic Burkitt lymphoma. PLoS Pathog. 2015;11:e1005158.
60. Kaymaz Y, Oduor CI, Yu H, Otieno JA, Ong'echa JM, Moormann AM, et al. Comprehensive transcriptome and mutational profiling of endemic Burkitt lymphoma reveals EBV type-specific differences. Mol Cancer Res. 2017;15:563–76.
61. Grande BM, Gerhard DS, Jiang A, Griner NB, Abramson JS, Alexander TB, et al. Genome-wide discovery of somatic coding and noncoding mutations in pediatric endemic and sporadic Burkitt lymphoma. Blood. 2019;133:1313–24.
62. Lin DC, Meng X, Hazawa M, Nagata Y, Varela AM, Xu L, et al. The genomic landscape of nasopharyngeal carcinoma. Nat Genet. 2014;46:866–71.
63. Wang K, Yuen ST, Xu J, Lee SP, Yan HH, Shi ST, et al. Whole-genome sequencing and comprehensive molecular profiling identify new driver mutations in gastric cancer. Nat Genet. 2014;46:573–82.
64. Piris MA, Medeiros LJ, Chang KC. Hodgkin lymphoma: a review of pathological features and recent advances in pathogenesis. Pathology. 2020;52:154–65.
65. Price AM, Messinger JE, Luftig MA. c-Myc represses transcription of the Epstein-Barr virus latent membrane protein 1 early after primary B cell infection. J Virol. 2018;92:e01178-17.
66. Jochner N, Eick D, Zimber-Strobl U, Pawlita M, Bornkamm GW, Kempkes B. Epstein-Barr virus nuclear antigen 2 is a transcriptional suppressor of the immunoglobulin mu gene: implications for the expression of the translocated c-myc gene in Burkitt's lymphoma cells. Embo J. 1996;15:375–82.
67. Kaiser C, Laux G, Eick D, Jochner N, Bornkamm GW, Kempkes B. The proto-oncogene c-myc is a direct target gene of Epstein-Barr virus nuclear antigen 2. J Virol. 1999;73:4481–4.
68. Bajaj R, Xu F, Xiang B, Wilcox K, Diadamo AJ, Kumar R, et al. Evidence-based genomic diagnosis characterized chromosomal and cryptic imbalances in 30 elderly patients with myelodysplastic syndrome and acute myeloid leukemia. Mol Cytogenet. 2011;4:3.
69. Kalchschmidt JS, Bashford-Rogers R, Paschos K, Gillman AC, Styles CT, Kellam P, et al. Epstein-Barr virus nuclear protein EBNA3C directly induces expression of AID and somatic mutations in B cells. J Exp Med. 2016;213:921–8.
70. Garcia-Gutierrez L, Bretones G, Molina E, Arechaga I, Symonds C, Acosta JC, et al. Myc stimulates cell cycle progression through the activation of Cdk1 and phosphorylation of p27. Sci Rep. 2019;9:18693.
71. Barreto V, Reina-San-Martin B, Ramiro AR, McBride KM, Nussenzweig MC. C-terminal deletion of AID uncouples class switch recombination from somatic hypermutation and gene conversion. Mol Cell. 2003;12:501–8.

ACKNOWLEDGEMENTS

The work was supported by grants PID2020-115903GB-100 to JL and MDD, RTI2018-095673-B-I00 to JRR, PID2019-107551RB-I00 to VG-Y, PID2020-119567RB-I00 to RM, PID2020-117539GB-I00 to IV and PID2019-106773RB-I00 to ARR, all funded by MCIN/AEI/10.13039/501100011033/, Spanish Government, and by "FEDER, Una manera de hacer Europa", European Union, and by La Caixa HR17-0244 grant to AR. LQ and VJ were recipients of F.P.U. program and Universidad de Cantabria fellowships, respectively. LG-G was a fellow of the Maria Zambrano program, Spanish Government. We are grateful to Maria Aramburu and Patricia Arribas for technical help, Santiago Montes for useful comments and Victor Campa por assistance in microscopy and image processing.

AUTHOR CONTRIBUTIONS

EM, LG-G: formal analysis, investigation, writing. VJ, MP-O, VG-Y, RB, AVM, JCA and LQ: formal analysis, investigation, resources. DU, RM, JRR, and IV: formal analysis and resources. IMA, AR: formal analysis, resources, editing. MDD: formal analysis, funding. JL: experimental design, formal analysis, writing, funding acquisition.

COMPETING INTERESTS

The authors declare no competing interests.

ADDITIONAL INFORMATION

Supplementary information The online version contains supplementary material available at https://doi.org/10.1038/s41388-023-02846-9.

Correspondence and requests for materials should be addressed to Javier León.

Reprints and permission information is available at http://www.nature.com/reprints

Publisher's note Springer Nature remains neutral with regard to jurisdictional claims in published maps and institutional affiliations.